

## Electronic Supplementary Information Section

### “Blackness” is an index of redox complexity in melanin polymers

Paola Manini,<sup>\*a</sup> Valeria Lino,<sup>a,b</sup> Gerardino D’Errico,<sup>a</sup> Samantha Reale,<sup>c</sup> Alessandra Napolitano,<sup>a</sup> Francesco De Angelis,<sup>c</sup> Marco d’Ischia<sup>a</sup>

Materials and methods	S2
Ammonia induced solid state polymerization (AISSP): general procedure	S2-S3
UV-vis spectrophotometric monitoring of the oxidation reaction of 1,6-DHN, 2,6-DHN and 2,7-DHN	S4-S5
UV-vis spectra of melanins from 1,8-DHN, 1,6-DHN, 2,6-DHN and 2,7-DHN as suspensions in DMF	S6
ATR spectrum of melanin powders from 1,6-DHN, 2,6-DHN and 2,7-DHN	S7-S8
MALDI mass spectra of melanins from 1,6-DHN, 2,6-DHN and 2,7-DHN and of polymers from 1-HN and 2-HN	S9
Comparison of the clusters of the $[M+Na]^+$ pseudomolecular ion peaks for synthetic melanins from 1-HN and 2-HN	S10
Melanin thin films on quartz substrates	S11
MALDI mass spectra of melanins thin films from 1,6-DHN, 2,6-DHN and 2,7-DHN obtained by AISSP	S12
EPR spectra of melanins from 1,8-DHN, 1,6-DHN, 2,6-DHN and 2,7-DHN and of polymers from 1-HN and 2-HN	S13-S14
Schematic picture of the redox complexity at each oligomeric stage	S15
Table S1. Thickness of the melanin thin films	S16

## Materials and methods

1,8-Dihydroxynaphthalene, 1,6-dihydroxynaphthalene, 2,6-dihydroxynaphthalene, 2,7-dihydroxynaphthalene, 1-naphthol, 2-naphthol, horseradish peroxidase (HRP, Type II, 150–250 EU/mg) and hydrogen peroxide were purchased from Sigma and used without further purification.

UV-Vis spectra were recorded with a Jasco V-560 instrument.

MALDI spectra were recorded on a Sciex 4800 MALDI ToF/ToF instrument using 2,5-dihydroxybenzoic acid as the matrix. The laser was operated at 3700 Hz in the positive reflectron mode. The mass spectrometer parameters were set as recommended by the manufacturer and adjusted for optimal acquisition performance. The laser spot size was set at medium focus (B50 mm laser spot diameter). The mass spectra data were acquired over a mass range of  $m/z$  100–4000 Da, and each mass spectrum was collected from the accumulation of 1000 laser shots. Raw data were analyzed using the computer software provided by the manufacturers and reported as monoisotopic masses.

Micro ATR spectra in transmission mode have been recorded with a Cary 660 FTIR Spectrometer with a Germanium crystal and a liquid nitrogen cooled Mercurium Cadmium Telluride (MCT) detector in the range from 4000 to 900  $\text{cm}^{-1}$ , with 32 scans both for background and samples, with a resolution of 4  $\text{cm}^{-1}$ .

Thin layer depositions were performed by spin coating using a Laurell WS-650MZ-23NPP/LITE spin coater.

Nine GHz EPR (X-band) spectra at room temperature were recorded on a Bruker Elexys E-500 spectrometer (Bruker, Rheinstetten, Germany). Capillaries containing the samples were flame sealed and placed in a standard 4 mm quartz sample tube. The instrumental settings were as follows: sweep width, 120 G; resolution, 1024 points; modulation frequency, 100 kHz; modulation amplitude, 1.0 G; time constant, 20.5 ms. From preliminary power saturation tests, a r.f. power level of 0.2 mW, was found to be sufficiently low to avoid saturation effects. Several scans, typically 4–16, were accumulated to improve the signal-to-noise ratio. Linewidths were measured from first-derivative curves (peak-to-peak distance expressed in G). The spin concentration was estimated by double integration of the experimental first-derivative spectrum, taking the ratio of area of the sample to that of a standard MgO-MnO solid solution, inserted co-axially in the standard sample tube. The g-value (Landé factor) was determined using the same standard.

## Ammonia induced solid state polymerization (AISSP): general procedure

A 100 mM solution of the proper dihydroxynaphthalene in methanol was prepared and filtered with 0.45  $\mu\text{m}$  syringe filters before use. For each deposition 100  $\mu\text{L}$  of the methanol solution of the selected dihydroxynaphthalene was pipetted on the upper side of the quartz substrate just before spinning. The spin coating programme was the following:  $\alpha$  = 500 rpm/s,  $\omega$  = 2000 rpm,  $t$  = 30 s. The dihydroxynaphthalene

coated substrate was placed in a glass chamber under an ammonia atmosphere equilibrated with air. After 24 h the polymerization was complete and the substrate was removed from the chamber.

The thickness of the mycomelanin thin films, determined with a Taylor Hobson CCI MP profilometer, are reported in Table S1.

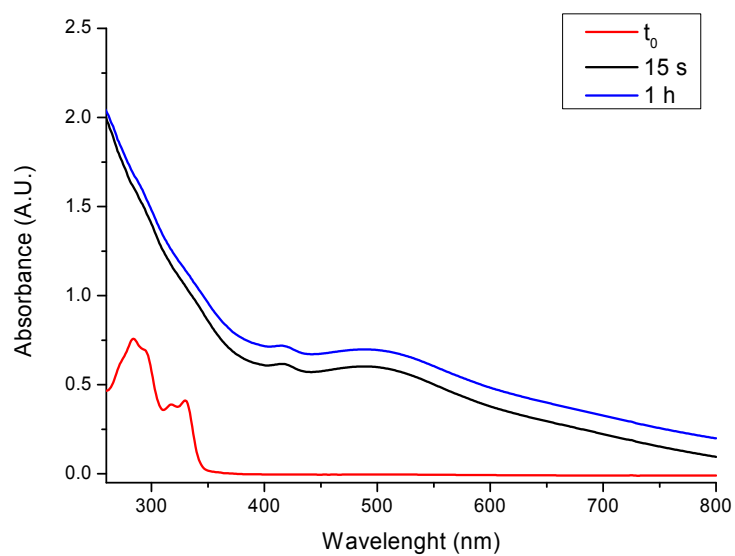


**Figure S1.** UV-vis spectrophotometric monitoring of the oxidation reaction of 1,6-dihydroxynaphthalene.

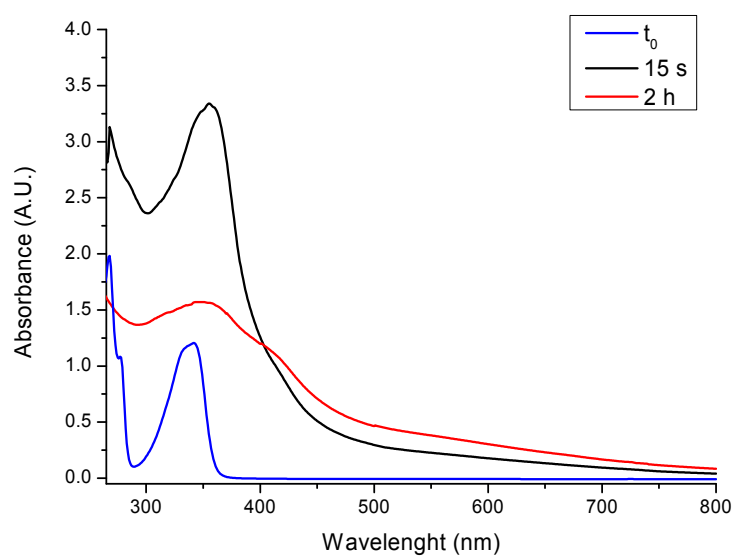


**Figure S2.** UV-vis spectrophotometric monitoring of the oxidation reaction of 2,6-dihydroxynaphthalene.

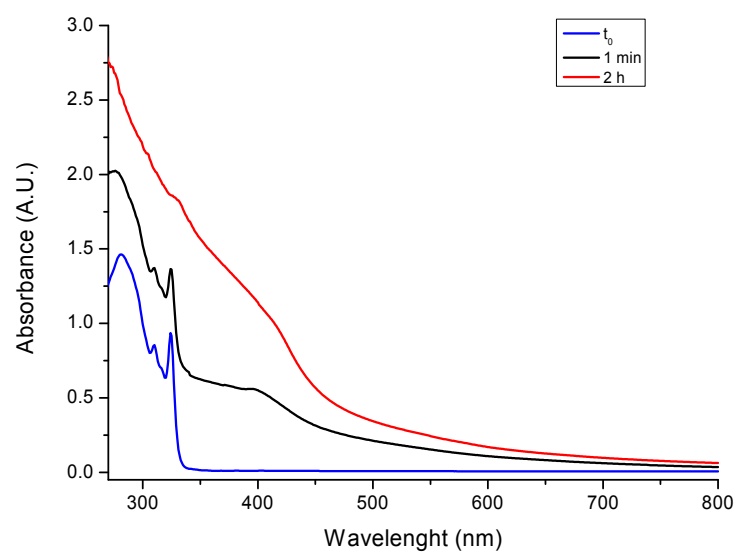


**Figure S3.** UV-vis spectrophotometric monitoring of the oxidation reaction of 2,7-dihydroxynaphthalene.

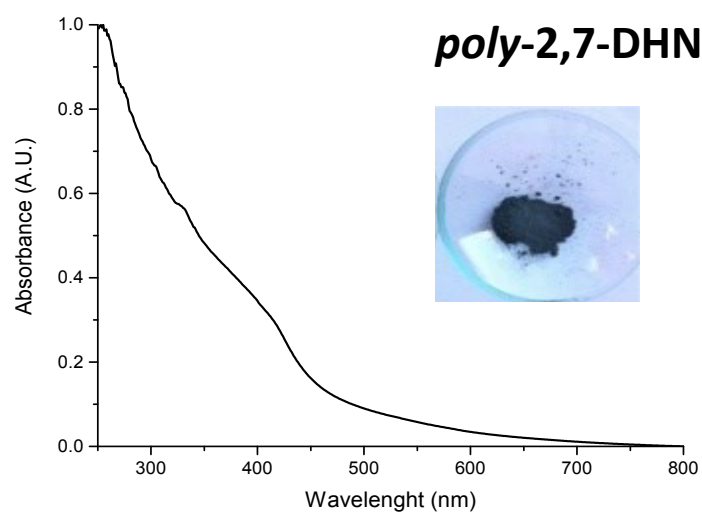
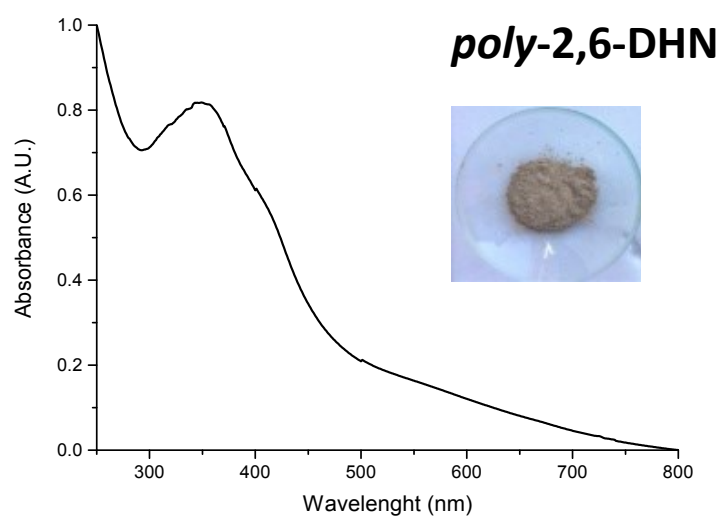
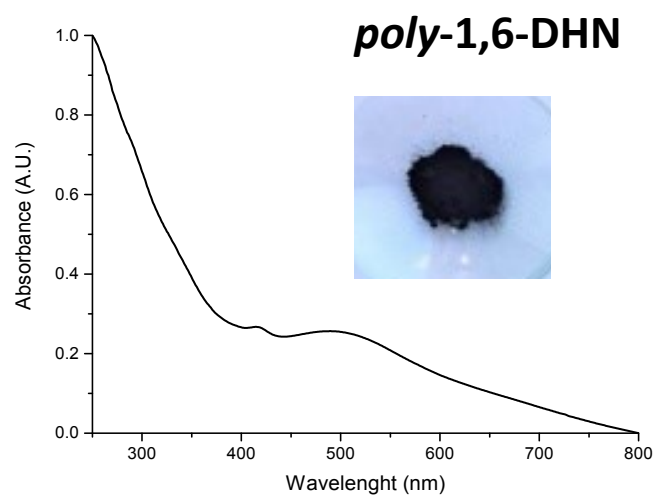


**Figure S4.** UV-vis spectra of synthetic melanins from 1,6-DHN, 2,6-DHN and 2,7-DHN as suspensions in DMF. Insets show the polymer powders.

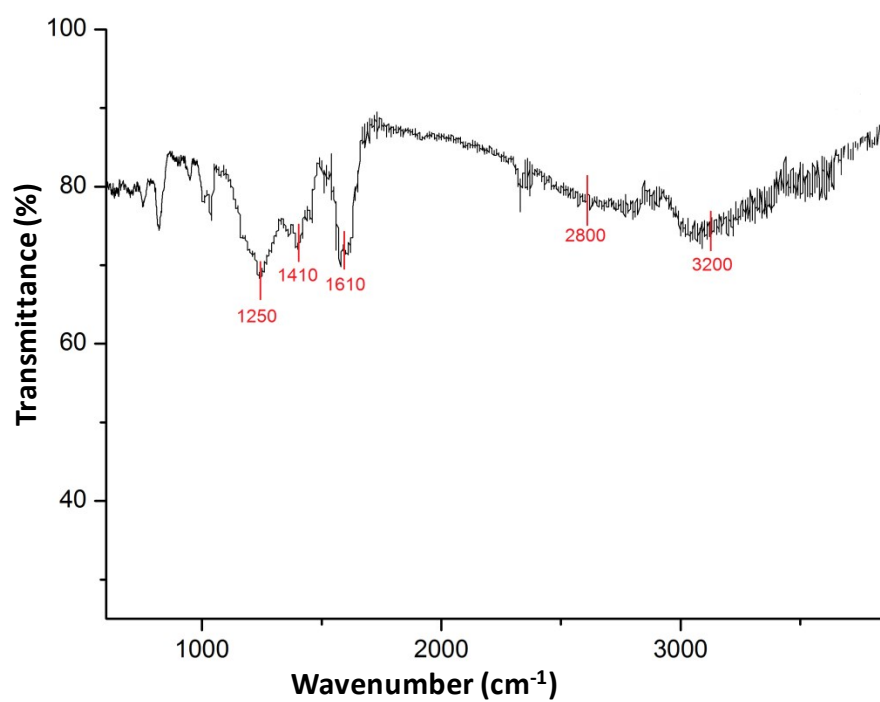


**Figure S5.** ATR spectrum of the synthetic melanin powder from 1,6-DHN.

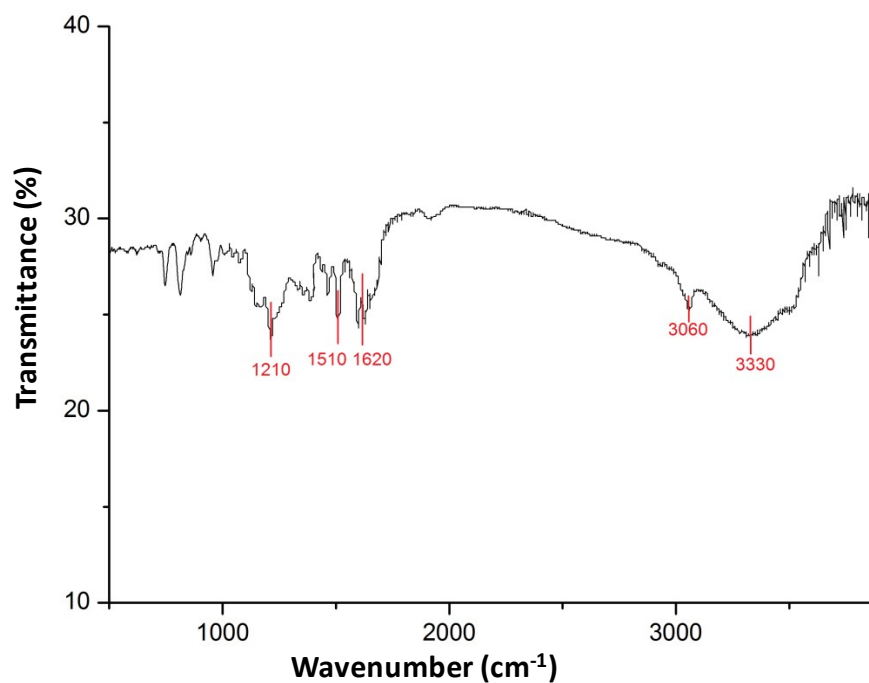


**Figure S6.** ATR spectrum of the synthetic melanin powder from 2,6-DHN.

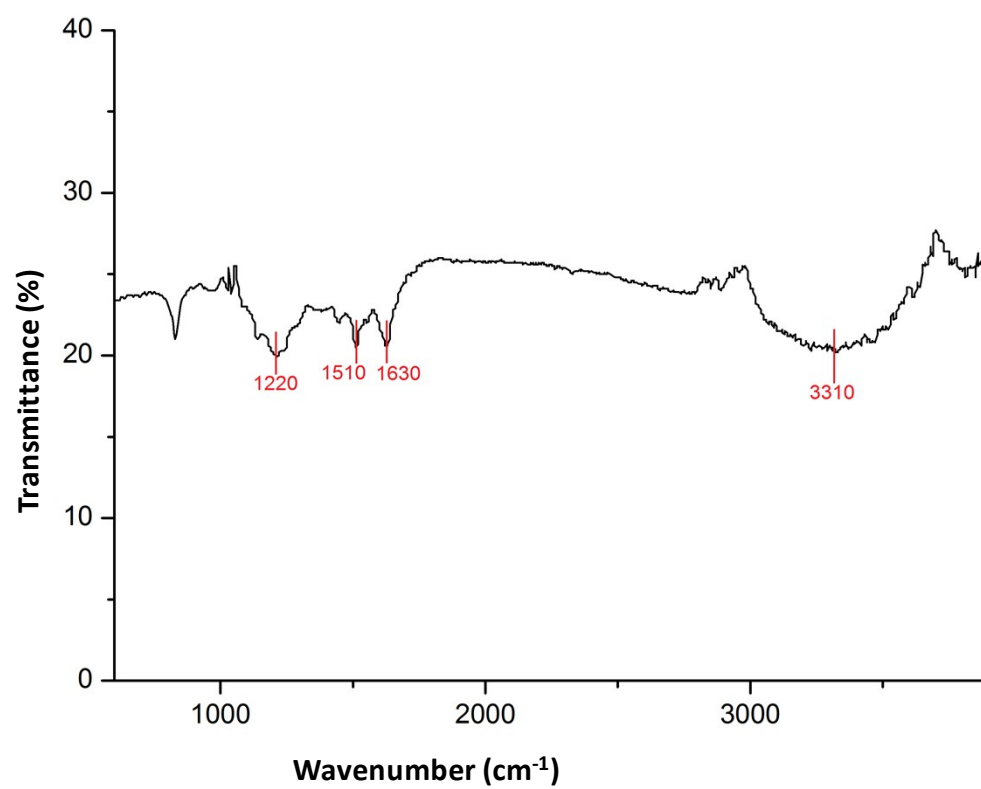


**Figure S7.** ATR spectrum of the synthetic melanin powder from 2,7-DHN.



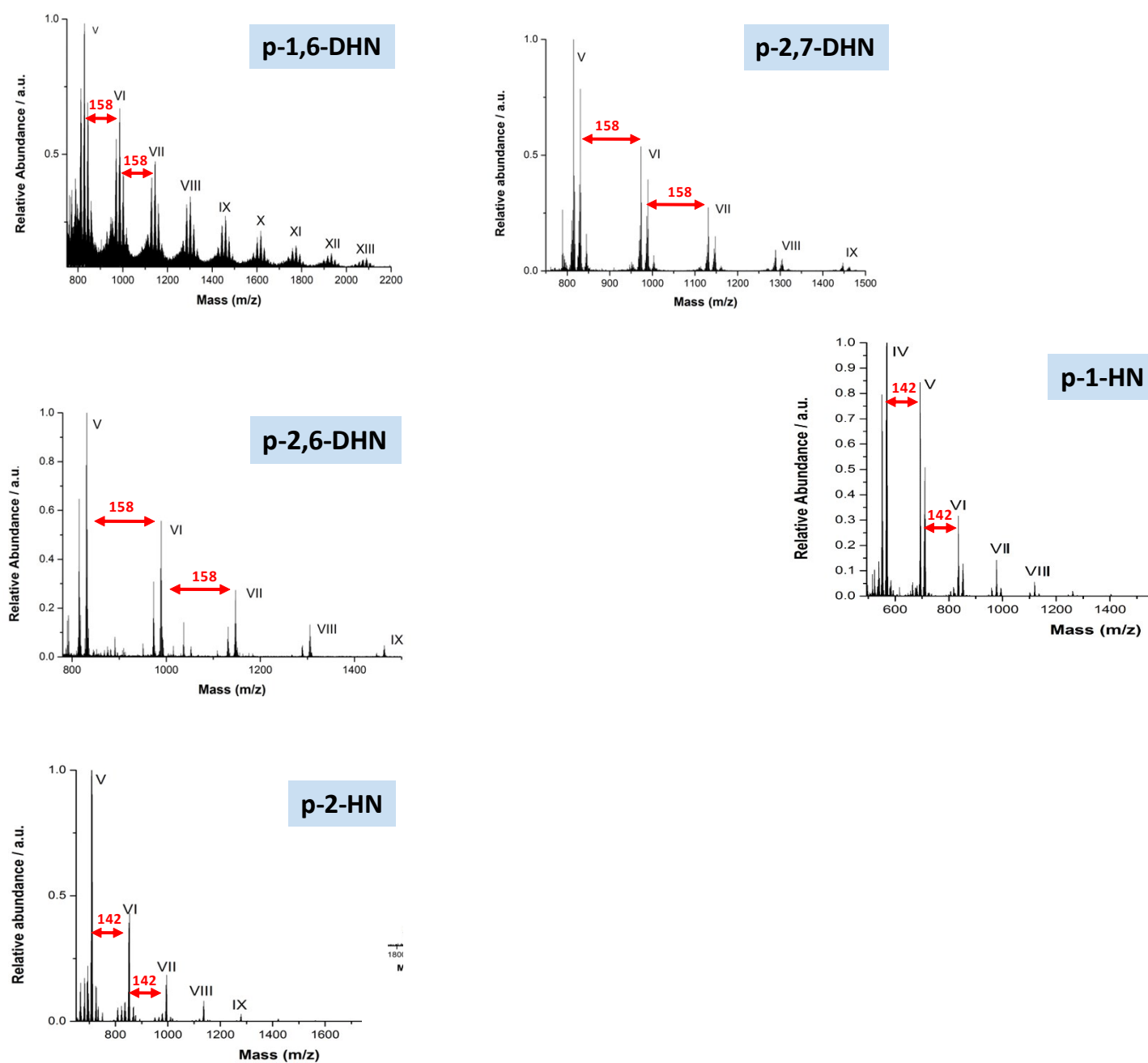


**Figure S8.** MALDI mass spectra of synthetic melanins from 1,6-DHN, 2,6-DHN and 2,7-DHN and of polymers from 1-HN and 2-HN.

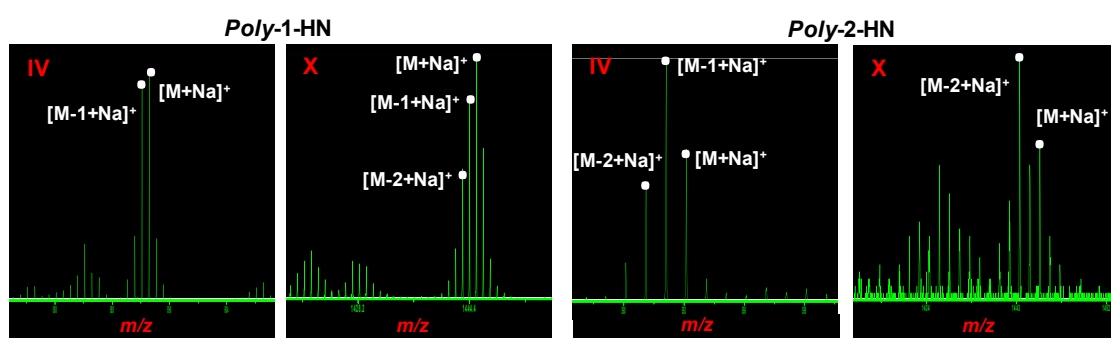


**Figure S9.** Comparison of the clusters of the  $[M+Na]^+$  pseudomolecular ion peaks for the 4-mer (IV) and 10-mer (X) oligomeric species of synthetic melanins from 1-HN and 2-HN.

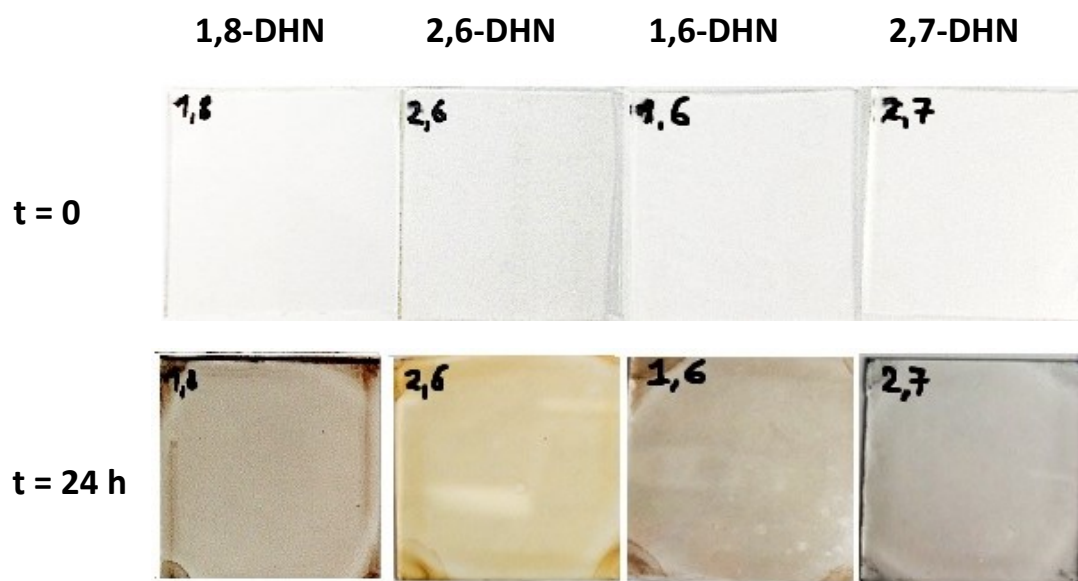
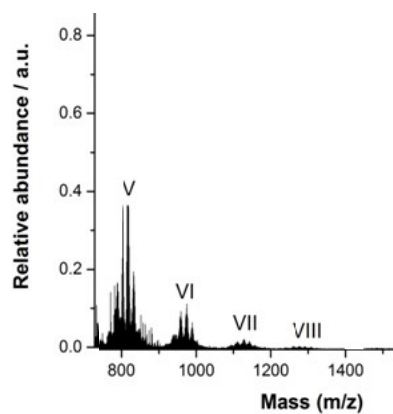
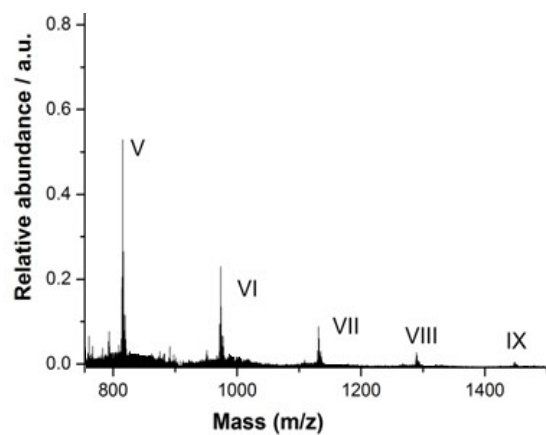


**Figure S10.** Dihydroxynaphthalene thin films on quartz substrates before (t = 0, top) and after (t = 24 h, bottom) exposure to air-equilibrated ammonia vapours.

***Poly-1,6-DHN thin film***



***Poly-2,6-DHN thin film***



***Poly-2,7-DHN thin film***

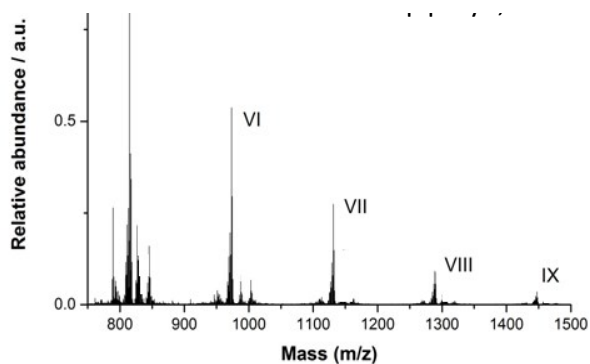


**Figure S11.** MALDI mass spectra of melanins thin films from 1,6-DHN, 2,6-DHN and 2,7-DHN obtained by AISSP.

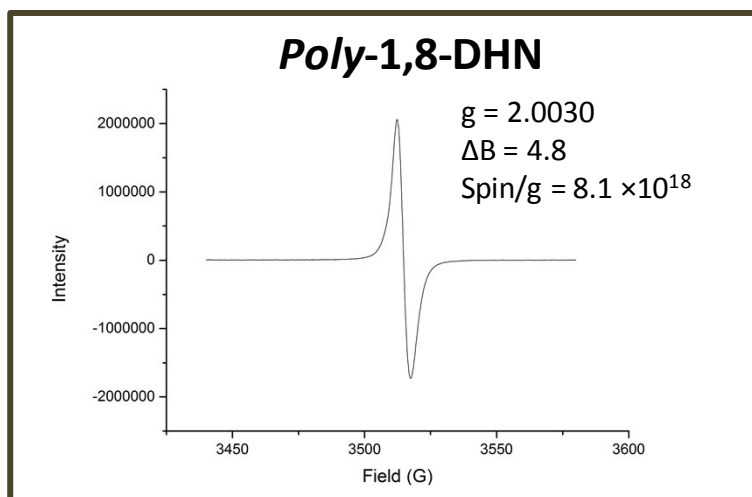


**Figure S12.** EPR spectrum of synthetic melanin from 1,8-DHN.

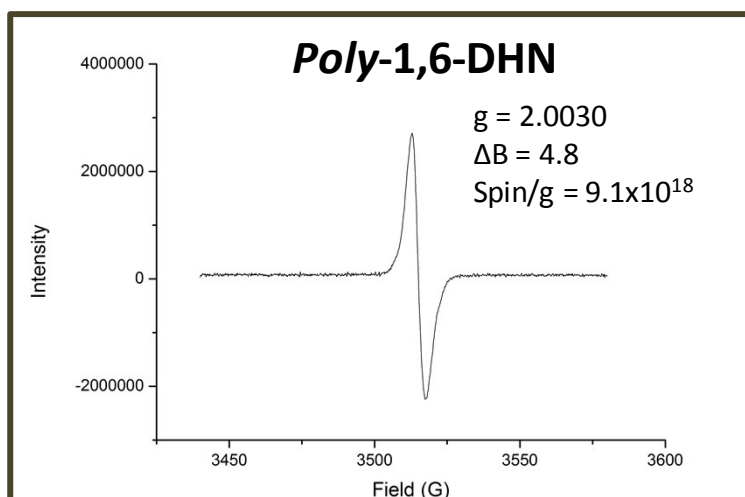


**Figure S13.** EPR spectrum of synthetic melanin from 1,6-DHN.

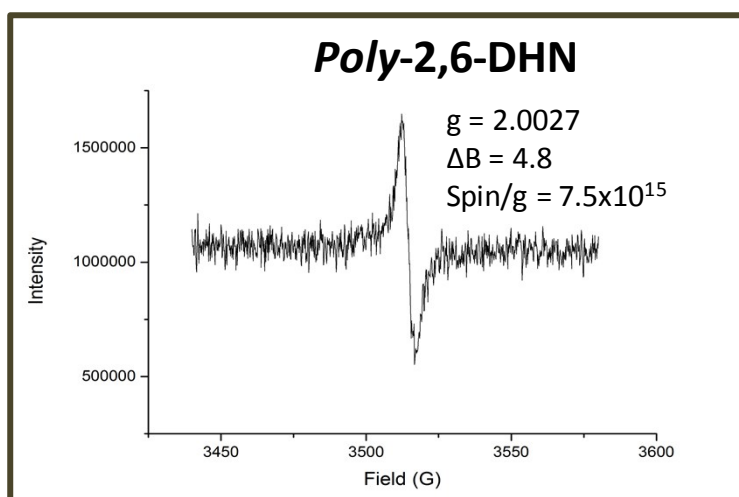


**Figure S14.** EPR spectrum of synthetic melanin from 2,6-DHN.

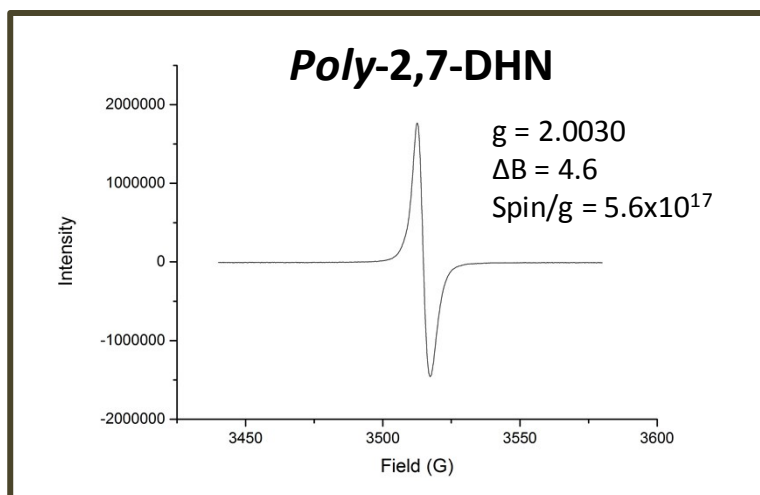


**Figure S15.** EPR spectrum of synthetic melanin from 2,7-DHN.

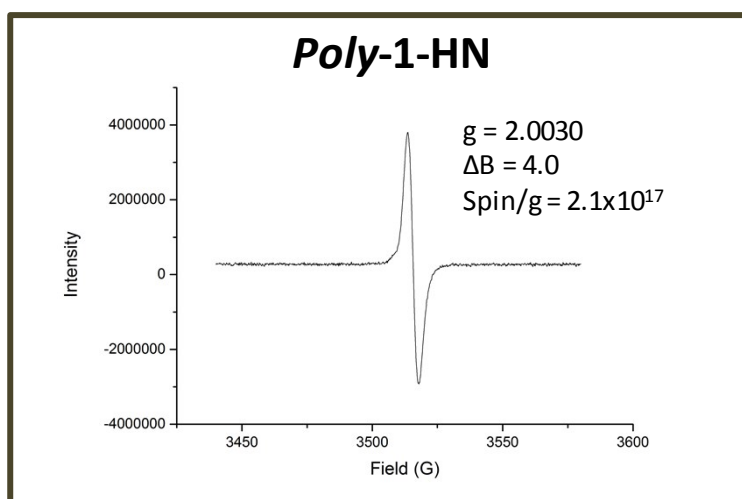


**Figure S16.** EPR spectrum of synthetic melanin from 1-HN.

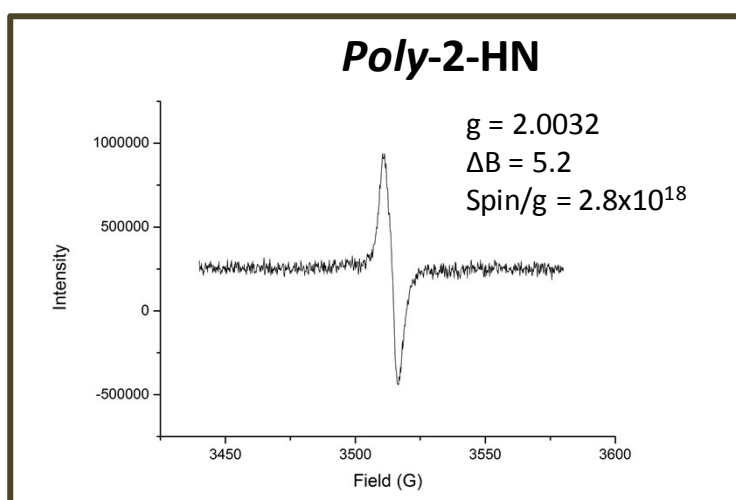


**Figure S17.** EPR spectrum of synthetic melanin from 2-HN.

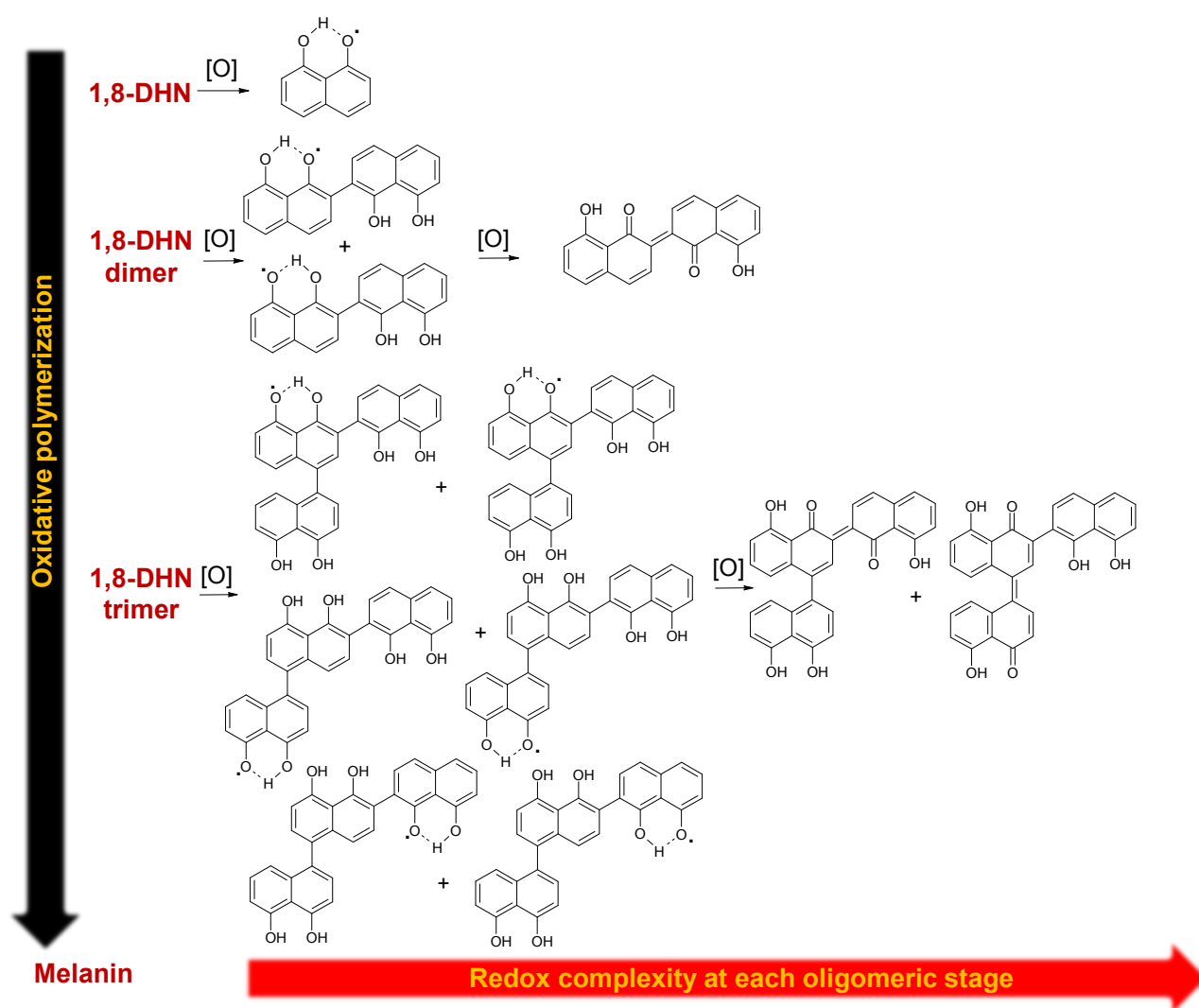


**Figure S18.** Schematic picture representing the the redox complexity at each oligomeric stage.

**Table S1. Thickness of the melanin thin films.**

	<b>Thickness (nm)</b>
<b>Poly-1,8-DHN</b>	130
<b>Poly-1,6-DHN</b>	132
<b>Poly-2,7-DHN</b>	132
<b>Poly-2,6-DHN</b>	129